Intramolecular Excited-State Processes of a Halato-Telechelic Polymer, Evaluated by Global Compartmental Analysis of the Fluorescence Decay Surface with the Use of Model Compounds

ARTICLE *in* MACROMOLECULES · SEPTEMBER 1997

Impact Factor: 5.8 · DOI: 10.1021/ma961271q

8 AUTHORS, INCLUDING:

Jan van Stam
Karlstads universitet
68 PUBLICATIONS **1,475** CITATIONS
SEE PROFILE

Frans C De Schryver
University of Leuven
670 PUBLICATIONS **21,277** CITATIONS
SEE PROFILE

Etienne Schacht
Ghent University
391 PUBLICATIONS **9,679** CITATIONS
SEE PROFILE

Intramolecular Excited-State Processes of a Halato-Telechelic Polymer, Evaluated by Global Compartmental Analysis of the Fluorescence Decay Surface with the Use of Model Compounds

Jan van Stam,[†] Frans C. De Schryver,*[,†] Noël Boens,[†] Bart Hermans,[†] Robert Jérôme,[‡] Geert Trossaert,[§] Erik Goethals,[§] and Etienne Schacht[§]

Departement Scheikunde, Katholieke Universiteit Leuven, Celestijnenlaan 200F, BE-3001 Heverlee, Belgium, Université de Liège, Sart Tilman, BE-4000 Liège, Belgium, and Universiteit Gent, BE-9000 Gent, Belgium

Received August 21, 1996; Revised Manuscript Received March 17, 1997[⊗]

ABSTRACT: The excited-state processes of the halato-telechelic polymer bis[(*N*,*N*-dimethyl-*N*-[3-(1-pyrenyl)propyl]ammonio)trifluoromethanesulfonate]-end-capped poly(tetrahydrofuran) at low concentrations are investigated by time-resolved fluorescence. The photophysical processes can be described by an intramolecular three-state excited-state model. Such a system is not identifiable in the absence of *a priori* information. It is possible to perform a global compartmental analysis of the fluorescence decay surface using the scanning technique, based on model compound data previously obtained [Hermans et al., *J. Phys. Chem.* **1994,** *98,* 13583 and Hermans et al. *Macromolecules* **1995,** *28,* 3380]. The value boundaries on the rate constant for ring closure of the chain ends show that this process is close to diffusion-controlled.

1. Introduction

Ionomers are polymers that are partly substituted by ionic residues, e.g., partially sulfonated poly(styrene)s. The introduction of ionic units drastically changes the properties of these materials,[1−4] and their behavior depends strongly on the dielectric constant of the solvent. In polar solvents the counterions will be readily solvated, resulting in a polymer backbone that covalently links several free charges. The importance of the electrostatic forces is reflected in the ionomer behavior in polar solvents, which is characterized as the polyelectrolyte behavior. In low-dielectric solvents ($\epsilon <$ 15), the counterions remain close to the ionic substituents of the polymer. Due to ion−ion interactions, contact ion pairs and/or solvent-separated ion pairs are formed,[5] which can be regarded as dipoles. In the literature, the formation of contact ion pairs is referred to as the ion-aggregate behavior.

Ionomers were initially studied by classical methods, e.g., viscometry[6−9] and light scattering.[10−12] The characteristic behavior of the reduced viscosity with the concentration in nonpolar solvents can generally be described in the following way. At low ionomer concentrations, the reduced viscosity is less than that of the corresponding neutral polymer. In this concentration regime, intrachain interactions are thought to be dominant. Increasing the concentration augments the reduced viscosity more steeply than the linear viscosity increase of the neutral polymer.[7] This is interpreted as the onset of the growing importance, and ultimately the predominance, of interchain associations.

Additional information on the aggregation was obtained by neutron scattering measurements.[13−16] The general picture is that most systems can be described by the open association model, in which a ground-state equilibrium is formed between single chains and aggregates of all sizes. SAXS and transmission electron microscopy were used to examine the occurrence of chain extension.[17] The microdomains formed by ionomers in nonpolar solvents were investigated in detail using different methods. Dowling and Thomas used the stopped-flow technique and found, for a partially sulfonated polystyrene ionomer, that the exchange of ionic materials could be described by a two-component, time-dependent, diffusion model.[18] They concluded that the ionic aggregates retained their intramolecular nature, even at high concentrations where intermolecular forces dominated the rheological characteristics.

Halato-telechelic polymers (HTP) are polymers end-capped with ionic functional groups. For simplicity, only linear HTP will be considered, thus carrying two ionic functional groups in the α and ω positions. α,ω-HTPs serve as model compounds for ionomers, as they show solvent polarity dependence similar to that of the ionomers, regardless of the fact that they only carry two ionic units.[8,11,19−25] The ion aggregation of HTPs in nonpolar solvents was closely examined by viscosity measurements,[4,20,21,26−28] and the same model, based on ion-pair aggregation, as proposed for ionomers,[22] is thought to be valid also for HTPs.

Depending on the concentration, intra- and interchain interactions will characterize the behavior of HTPs. One way to probe these association interactions is to measure excimer formation of an attached fluorescence probe.[29] This can be done by the substitution of an ionic probe moiety in the α and/or ω positions of the polymer chain. Pyrene excimer formation has widely been used for this purpose in the study of neutral polymer association phenomena,[30] focusing on, e.g., viscosity,[31,32] solvent effects,[33] temperature effects,[34] kinetics,[35,36] thermodynamics,[37] and ground-state equilibria.[38,39] Telechelic polymers, however, have been investigated much less by this method, and only a few investigations are reported.[40−42] For HTPs, only one report is, to our knowledge, found in the literature.[29]

It should be noted that all models presented, and all data confirming these models, describe a static view of the ion-aggregation behavior. By time-resolved fluorescence spectroscopy it is possible to obtain detailed

* To whom correspondence should be addressed. E-mail address: Frans.DeSchryver@Chem.KULeuven.ac.be.
[†] Katholieke Universiteit Leuven.
[‡] Université de Liège.
[§] Universiteit Gent.
[⊗] Abstract published in *Advance ACS Abstracts,* September 1, 1997.

S0024-9297(96)01271-5 CCC: $14.00

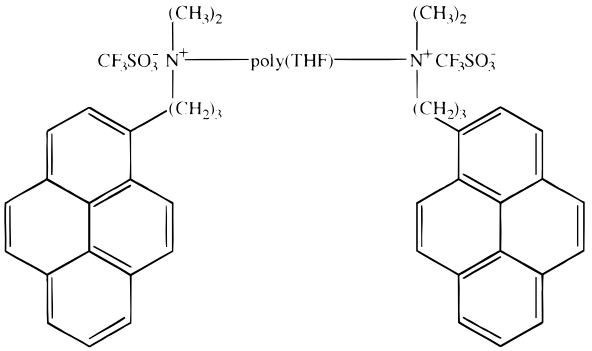

Figure 1. α,ω-Halato-telechelic polymer bis[(*N*,*N*-dimethyl-*N*-[3-(1-pyrenyl)propyl]ammonio)trifluoromethanesulfonate]-end-capped poly(tetrahydrofuran) (POLYDIPROBE).

kinetic information about the excited-state processes.

To fully understand the information obtained by time-resolved fluorescence measurements of an at both chain ends probe-capped polymer, the kinetic behavior of the probe itself has to be elucidated. Furthermore, for the determination of the excited-state kinetics of an HTP, it is advantageous to study the single chain end-capped polymer in a preceding step. Global compartmental analysis[43−52] provides the opportunity to determine all rate constants and spectroscopic parameters in a single step and has successfully been applied to a number of systems.[53−60]

In previous articles, the kinetics of the charged fluorescent probe *N*,*N*,*N*-trimethyl-3-(1-pyrenyl)-1-propanaminium perchlorate (PROBE[61]) and (*N*,*N*-dimethyl-*N*-[3-(1-pyrenyl)propyl]ammonio)trifluoromethanesulfonate-end-capped poly(tetrahydrofuran) (POLYPROBE[62]) were unraveled. Based on a kinetic scheme in which dipole−dipole association and excimer formation are taken into account, it was possible to determine all the rate constants within certain value boundaries. In the present step, we extend the study to a HTP, bis[(*N*,*N*-dimethyl-*N*-[3-(1-pyrenyl)propyl]ammonio)(trifluoromethanesulfonate)]-end-capped poly(tetrahydrofuran). By the use of the previously obtained results,[61,62] and performing an analysis of the fluorescence decay surface using the scanning technique,[47,48,58,62] it is possible to determine the rate constants within certain value boundaries for the intramolecular excited-state ring-closure and ring-opening processes.

2. Experimental Section

2.1. Materials and Data Analysis. Tetra-*tert*-butylammonium perchlorate (*t*-BUTAP) was from FLUKA, and tetrahydrofuran (THF, HPLC grade) was supplied by Rathburn. Both were used as received.

2.2. Synthesis and Characteristics of Bis[(*N*,*N*-dimethyl-*N*-[3-(1-pyrenyl)propyl]ammonio)trifluoromethanesulfonate]-End-Capped Poly(tetrahydrofuran) (POLYDIPROBE). Bis[(*N*,*N*-dimethyl-*N*-[3-(1-pyrenyl)propyl]ammonio)trifluoromethanesulfonate]-end-capped poly(tetrahydrofuran) (POLYDIPROBE) was synthesized in the same way as POLYPROBE,[62] but with the bifunctional triflate anhydride ($(CF_3SO_2)O$) as initiator. Polytetrahydrofuran was synthesized via cationic ring-opening polymerization with methyl triflate ($CF_3SO_3CH_3$) as initiator.

The characteristics for POLYDIPROBE are M_n(GPC) 5620, M_w(GPC) 6230, M_w(NMR) 6430. The structure of POLYDIPROBE is shown in Figure 1.

2.3. Fluorescence Measurements. Corrected steady-state emission spectra ($\lambda_{ex} = 320$ nm) were recorded on a SPEX Fluorolog 1680 combined with a SPEX Spectroscopy Laboratory Coordinator DM1B (band-pass 2 nm) in the right-angle mode.

Scheme 1

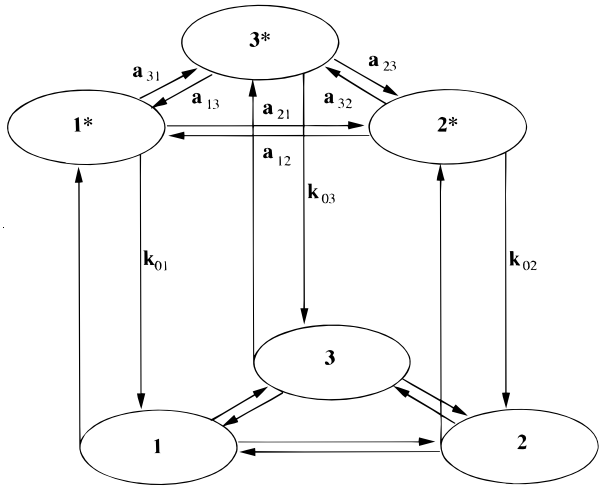

Fluorescence decays were obtained by use of a Spectra-Physics mode-locked, synchronously pumped, cavity-dumped, frequency-doubled DCM dye laser as the excitation source ($\lambda_{ex} = 320$ nm) with single-photon counting detection. A detailed description of the equipment has been given elsewhere.[63,64] The decays were collected at several wavelengths between 375 and 500 nm, all observed at the magic angle (54.7°), and contained 10 000 (longer time/channel) or 5000 (shorter time/channel) peak counts. The details about the measurements on PROBE[61] and POLYPROBE[62] are given elsewhere. For POLYDIPROBE, the decays were collected in 512 channels of the multichannel analyzer at four different emission wavelengths, 375, 395, 480, and 500 nm, and with two different time increments, 408 ps/channel and 1.185 ns/channel. The concentration of POLYDIPROBE was 1 μM, using M_w(GPC) as molecular weight. 9-Cyanoanthracene in methanol was used as the reference compound ($\tau_{ref} = 16.7$ ns) for the reference convolution[65] of the fluorescence decays.

All solutions for fluorescence measurements were prepared in THF, and the sample solutions in 1 × 1 cm cells were degassed using five freeze−pump−thaw cycles prior to the measurements. All measurements were performed at 20 °C.

3. Theory and Data Analysis

3.1. Excited-State Processes in Compartmentalized Systems. Solely systems without an added fluorescence quencher will be discussed here; for systems with an added quencher, both theory[46,48] and experimental[44,58−60] work have been reported. The theory of global compartmental analysis of fluorescence decay surfaces is thoroughly described,[43−52,61,62] and only the fundamental aspects of tricompartmental systems will briefly be summarized. The special case of an *intramolecular* tricompartmental system will be discussed in detail.

3.2. Tricompartmental Systems without Added Quencher. Consider a general tricompartmental system, depicted in Scheme 1. Compartments 1 and 2 are two different locally excited states, while compartment 3 will be assigned to the excimer state. After excitation, which does not significantly alter the ground-state concentrations, the fluorescence δ-response function, $f(\lambda_{ex},\lambda_{em},t)$, at emission wavelength λ_{em} due to excitation at λ_{ex}, is given by[43]

$$f(\lambda_{ex},\lambda_{em},t) = \mathbf{c}(\lambda_{em})\ \mathbf{U}\ \exp(t\Gamma)\ \mathbf{U}^{-1}\ \mathbf{b}(\lambda_{ex}) \qquad (1)$$

U is the matrix of the eigenvectors of matrix **A** (vide infra), and $\mathbf{U}^{-1}$ is the inverse of **U**. $\mathbf{b}(\lambda_{ex})$ is the vector of the excited-state concentrations at time zero, and it is independent of the emission wavelength. $\mathbf{c}(\lambda_{em})$ is the

vector of the spectral emission weight factors $c_i(\lambda_{em})$ of species i^* at λ_{em}, which are dependent on the emission wavelength only.

Defining the normalized elements $\tilde{b}_i$ and $\tilde{c}_i$ as

$$\tilde{b}_i = \frac{b_i}{\sum_{\forall i} b_i} \tag{2}$$

and

$$\tilde{c}_i = \frac{c_i}{\sum_{\forall i} c_i} \tag{3}$$

allows a modified form of eq 1:

$$f(\lambda_{ex},\lambda_{em},t) = \kappa \tilde{\mathbf{c}}(\lambda_{em})\, \mathbf{U} \exp(t\Gamma)\, U^{-1}\, \tilde{\mathbf{b}}(\lambda_{ex}) \tag{4}$$

with κ a proportionality constant (or scaling factor). **U** will be given by $\mathbf{U} \equiv [\mathbf{U}_1,\mathbf{U}_2,\mathbf{U}_3]$, γ_1, γ_2, and γ_3 are the eigenvalues of **A** corresponding to $\mathbf{U}_1$, $\mathbf{U}_2$, and $\mathbf{U}_3$, respectively, and $\exp(t\Gamma) \equiv \mathrm{diag}[\exp(\gamma_1 t), \exp(\gamma_2 t), \exp(\gamma_3 t)]$. The compartmental matrix **A** is defined as

$$\mathbf{A} \equiv \begin{bmatrix} -(k_{01}+a_{21}+a_{31}) & a_{12} & a_{13} \\ a_{21} & -(k_{02}+a_{12}+a_{32}) & a_{23} \\ a_{31} & a_{32} & -(k_{03}+a_{13}+a_{23}) \end{bmatrix} \tag{5}$$

The excited-state species can decay by fluorescence (F) and nonradiative processes (NR). The composite rate constant of the decay of species i^* is denoted k_{0i}, with $k_{0i} = k_{Fi} + k_{NRi}$. The excited-state interconversion from state j^* to i^* ($j^* \rightarrow i^*$), as described by matrix element a_{ij} and the corresponding rate constants, is given by k_{ij} ($a_{ij} = k_{ij}$ for an intramolecular process and $a_{ij} = k_{ij}[M]$ for an intermolecular process, where [M] is the concentration in the reaction $j^* + M \rightarrow i^*$).

$\tilde{\mathbf{c}}(\lambda_{em})$ and $\tilde{\mathbf{b}}(\lambda_{ex})$ will, for a tricompartmental system, be defined as

$$\tilde{\mathbf{b}} = \begin{bmatrix} \tilde{\mathbf{b}}_1 \\ \tilde{\mathbf{b}}_2 \\ 1 - (\tilde{\mathbf{b}}_1 + \tilde{\mathbf{b}}_2) \end{bmatrix} \tag{6a}$$

$$\tilde{\mathbf{c}} = [\tilde{c}_1 \quad \tilde{c}_2 \quad 1 - (\tilde{c}_1 + \tilde{c}_2)] \tag{6b}$$

Equation 1 can be written in the triple-exponential form:

$$f(\lambda_{ex},\lambda_{em},t) = \sum_{i=1}^{3} \alpha_i \exp(\gamma_i t) \tag{7}$$

To proceed, some assumptions will be made in order to simplify the general tricompartmental system. First, assume the interconversions $1^* \rightarrow 2^*$ and $1^* \rightarrow 3^*$ to be bimolecular for *intermolecular* processes and to be described by the second order rate constants k_{21} and k_{31}, respectively, while for *intramolecular* processes they are described by first-order rate constants. Second, the processes $2^* \rightarrow 1^*$ and $2^* \rightarrow 3^*$ are assumed to be monomolecular and described by the first-order rate constants k_{12} and k_{32}, respectively. Final, the interconversions $3^* \rightarrow 1^*$ and $3^* \rightarrow 2^*$ are presumed to be negligibly slow. These assumptions simplify Scheme 1 to Scheme 2 and the compartmental matrix **A** will be given by

Scheme 2

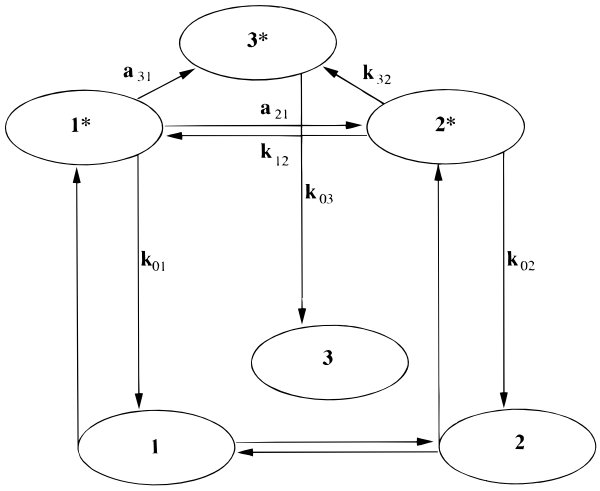

$$\mathbf{A} \equiv \begin{bmatrix} -(k_{01} + a_{21} + a_{31}) & k_{12} & 0 \\ a_{21} & -(k_{02} + k_{12} + k_{32}) & 0 \\ a_{31} & k_{32} & -k_{03} \end{bmatrix} \tag{8}$$

The exponential factors γ_i are related to the decay times in the same way as for a bicompartmental system[43-45,47] and are explicitly given for the model depicted in Scheme 2 by $\gamma_1 = -k_{03}$ and $\gamma_{2,3}$ given by

$$\gamma_{1,2} = -\frac{1}{2}(S_1 + S_2 \pm \sqrt{(S_1 - S_2)^2 + 4P}) \tag{9}$$

with

$$S_1 = k_{01} + a_{21} + a_{31} \tag{10a}$$

$$S_2 = k_{02} + k_{12} + k_{32} \tag{10b}$$

$$P = a_{21}k_{12} \tag{10c}$$

In eqs 10, a_{21} and a_{31} equal $k_{21}[M]$ and $k_{31}[M]$, respectively, for intermolecular processes and k_{21} and k_{31}, respectively, for intramolecular processes.

From the explicit expressions of the decay times for this kind of system, it follows that only one of the measured decay times ($\tau_3 = -1/k_{03}$) is directly related to one excited-state species. The other two will be functions of the remaining rate constants of the excited-state system (and the concentration of reactant M for an intermolecular system) and cannot be related to a particular excited state. For intermolecular systems this offers a possibility to determine one of the kinetic parameters. Plots of the measured decay times as a function of [M] will give the rate constant k_{03}, as this rate constant equals the inverse of the concentration-independent decay time. The variation of the two remaining decay rates can, for an intermolecular system, be used for the determination of the remaining rate constants if the decays are collected at different concentrations of M.[49,61]

3.3. Special Case: Intramolecular Tricompartmental System without Added Quencher. In this section, we will treat the special case of an *intramolecular* tricompartmental system without added

Scheme 3

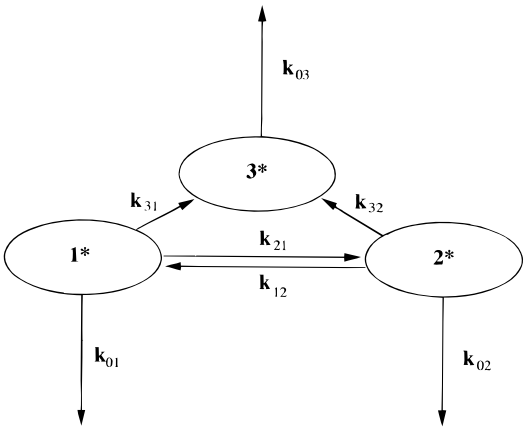

quencher and with negligible return paths from one of the excited-state compartments to the other two compartments. This special case is depicted in Scheme 3, with k_{13} and k_{32} both equal to zero.

For this kind of systems, the compartmental matrix **A** will be given by

$$\mathbf{A} \equiv \begin{bmatrix} -(k_{01} + k_{21} + k_{31}) & k_{12} & 0 \\ k_{21} & -(k_{02} + k_{12} + k_{32}) & 0 \\ k_{31} & k_{32} & -k_{03} \end{bmatrix} \tag{11}$$

For an intramolecular tricompartmental system as depicted in Scheme 3, no use can be made of the variation of reactant concentrations—all rate constants are first-order and the decay times will be independent of concentration, which leads to identifiability problems. For the case of *intermolecular* tricompartmental systems, an identifiability study has been performed,[61] which we will use as the starting point for the identifiability study of an *intramolecular* system.

For an intramolecular system as depicted in Scheme 3, the basic equations, similar to an intermolecular system, are

$$\sigma_1 = \sum_{\forall i} \gamma_i = -(S_1 + S_2 + k_{03}) \tag{12a}$$

$$\sigma_2 = \sum_{i<j} \gamma_i \gamma_j = S_1 S_2 + k_{03}(S_1 + S_2) - P \tag{12b}$$

$$\sigma_3 = \sum_{i<j<k} \gamma_i \gamma_j \gamma_k = (P - S_1 S_2) k_{03} \tag{12c}$$

with S_1, S_2, and P given by eqs 10. Since k_{03} is assumed to be known (vide infra), σ_3 can be written as a linear combination of σ_1 and σ_2:

$$\frac{\sigma_3}{k_{03}} = -\{\sigma_2 + k_{03}(\sigma_1 + k_{03})\} \tag{13}$$

from which one obtains two linearly independent equations:

$$-(\sigma_1 + k_{03}) = S_1 + S_2 = k_{01} + k_{21} + k_{31} + k_{02} + k_{12} + k_{32} \tag{14a}$$

$$\frac{\sigma_3}{k_{03}} = P - S_1 S_2 = -\{k_{21}(S_2 - k_{12}) + (k_{01} + k_{31}) S_2\} \tag{14b}$$

If k_{02}, k_{12}, and k_{32} are known, S_2 is determined, and if, additionally, k_{01} is known, eqs 14 can be written as

$$\sigma_1 + k_{01} + k_{03} + S_2 = -(k_{21} + k_{31}) \tag{15a}$$

$$\frac{\sigma_3}{k_{03}} + k_{01} S_2 = -[(S_2 - k_{12}) k_{21} + S_2 k_{31}] \tag{15b}$$

For each value of k_{32}, one obtains a new value of S_2 and, consequently, a new system of two equations linear in k_{21} and k_{31} (eqs 15). In other words, for each value of k_{32}, one can compute values of k_{21} and k_{31}. Hence, the model depicted in Scheme 3 is identifiable if k_{01}, k_{02}, k_{12}, and k_{32} are assumed to be known.

Scanning the rate constant k_{32}, i.e., k_{32} is repetitively held constant at different preset values, allows one to determine the value boundaries of the rate constants k_{21} and k_{31}.[47,48,58,62] Eqs 14 predict that plotting $S_1 + S_2$ and $P - S_1S_2$ *vs* k_{32} should yield plateaus from which the average values $\overline{S_1 + S_2}$ and $\overline{P - S_1S_2}$ can be determined.

The maximum and minimum values of k_{32} can be determined from the scanning procedure. There are two ways to determine the value boundaries on the unknown rate constants k_{21} and k_{31}. First, the values of k_{21} and k_{31} obtained from the scanning procedure can be plotted as a function of k_{32}, from which the value boundaries of k_{21} and k_{31} can be estimated. Alternatively, if one substitutes $\overline{S_1 + S_2}$ for $-(\sigma_1 + k_{03})$ and $\overline{P - S_1S_2}$ for σ_3/k_{03} in eqs 15, k_{21} and k_{31} can be calculated for each value of the scanned rate constant k_{32}, yielding value boundaries on k_{21} and k_{31}.

3.4. Data Analysis. Compartmental analysis is by definition global,[66−70] and the parameters of eq 4 can be common for all experimental data, e.g., k_{ij}, which are *globally* linked over the whole decay surface, or common only for a part of the data, e.g., $\tilde{\mathbf{c}}$, which is common for all decays collected at the same λ_{em}, which are *regionally* linked. The only local parameter is the scaling factor κ.

Consider the excited-state processes depicted by Schemes 1−3. The global and regional fitting parameters are k_{ij}, $\tilde{\mathbf{c}}(\lambda_{em})$, and $\tilde{\mathbf{b}}(\lambda_{ex})$ and the only local fitting parameters are the scaling factors. Using this approach, experiments done at different excitation/emission wavelengths, at multiple timing calibrations, and at different concentrations are linked by all rate constants defining the system.

The global compartmental analysis program, based on Marquardt's algorithm,[71] has been described elsewhere.[63,70] All calculations were performed on an IBM 6000 RISC computer.

The fitting parameters were estimated by minimizing the global reduced χ_g^2:

$$\chi_g^2 = \sum_{l}^{q} \sum_{i} w_{li} (y_{li}^{o} - y_{li}^{c})^2 / \nu \tag{16}$$

where index l sums over q experiments and index i sums over the appropriate channels for each individual experiment. y_{li}^{o} and y_{li}^{c} denote the observed (experimentally measured) and calculated (fitted) values corresponding to the ith channel of the lth experiment, respectively, and w_{li} is the corresponding statistical weight (a Poissonian distribution is assumed). ν represents the number of degrees of freedom for the entire multidimensional fluorescence decay surface.

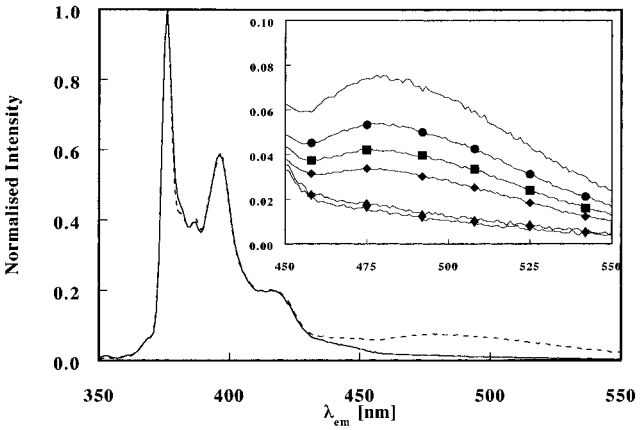

Figure 2. Normalized stationary emission spectra of POLYDIPROBE (1 μM in THF) at varying *t*-BUTAP concentrations. Main figure: (dashed line) 0 mM *t*-BUTAP; (full line) 250 mM *t*-BUTAP. The inserted figure shows the excimer region: (no marker) 0 mM *t*-BUTAP; (●) 10 mM *t*-BUTAP; (■) 25 mM *t*-BUTAP; (◆) 50 mM *t*-BUTAP; (▲) 125 mM *t*-BUTAP; (▼) 250 mM *t*-BUTAP.

The statistical criteria to judge the quality of the fit include both graphical and numerical tests. The graphical methods comprised plots of surfaces of the autocorrelation function values vs experiment number and of the weighted residuals vs channel number vs experiment number. The numerical statistical tests incorporated the calculation of χ_g^2 and its corresponding $Z(\chi^2)$:

$$Z(\chi^2) = (\chi_g^{\,2} - 1)\sqrt{\nu/2} \qquad (17)$$

Fits for which $Z(\chi^2) \leq 5$ were regarded as good. The additional statistical criteria to judge the quality of the fit are described elsewhere.[72]

4. Results and Discussion

The halato-telechelic polymer POLYDIPROBE, which can form ion−ion aggregates and excimers intramolecularly, is shown in Figure 1. The possibility of intramolecularly ring-closure was not available in the POLYPROBE system. From the investigations of PROBE[61] and POLYPROBE,[62] the rate constants of the intermolecular processes are known. POLYDIPROBE offers the possibility to study the *intramolecular* processes without contribution of intermolecular processes. The emphasis will be put on the interconversions between the ring-opened and the ring-closed states. For this reason, measurements on POLYDIPROBE were only performed at low POLYDIPROBE concentrations, [POLYDIPROBE] = 1 μM. At this concentration, all processes are intramolecular and described by Scheme 2 with all rate constants being first-order. The goal is to estimate the values of the rate constants of Scheme 2, based on the results from the two model compounds PROBE[61] and POLYPROBE[62] and through global compartmental analysis.

4.1. Stationary Measurements. Stationary emission spectra of POLYDIPROBE were measured at different concentrations of *t*-BUTAP, ranging from 0 to 250 mM. The spectra show the typical emission of a pyrene excimer, with a maximum around 480 nm, Figure 2. Adding the quaternary ammonium salt *t*-BUTAP to the solutions, screens the electrostatic attraction, causing the ion−ion aggregation and the excimer formation, but even at the highest salt concentration, [*t*-BUTAP] = 250 mM, a weak excimer emission is detected (see inserted magnification in Figure 2).

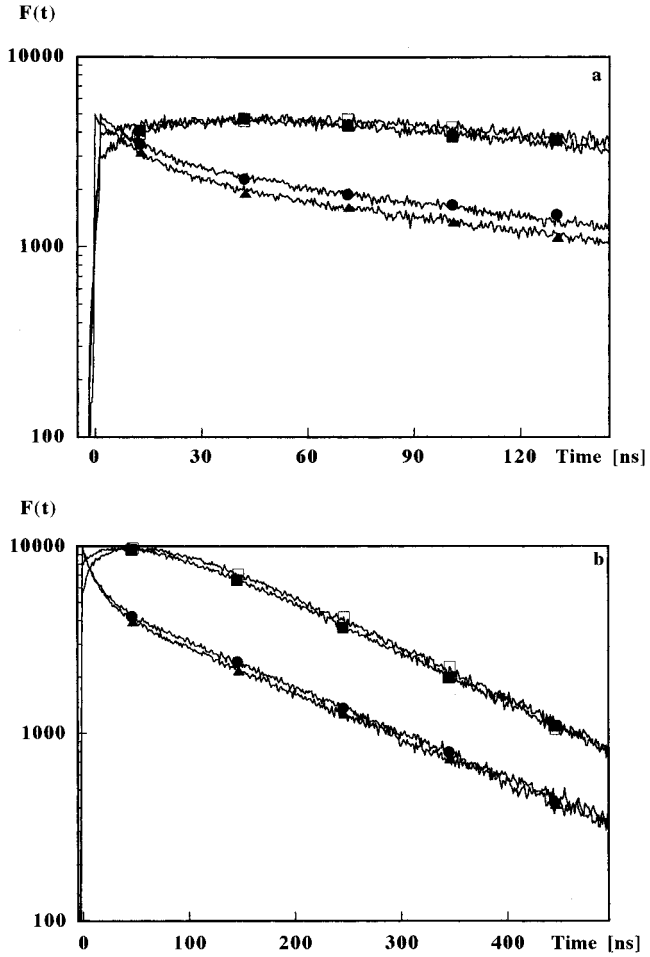

Figure 3. Fluorescence decays of 1 μM POLYDIPROBE in THF, excited at 320 nm at different emission wavelengths, (▲) 375 nm; (●) 395 nm; (■) 480 nm; (□) 500 nm, and collected at two different time increments, **(**a**)** 408 ps/channel and **(**b**)** 1.185 ns/channel.

4.2. Time-Resolved Measurements. The time-resolved fluorescence measurements were performed with two different time increments and the emission was collected at four different wavelengths. The collected emission decay profiles are shown in Figure 3, and the decay rates obtained are independent of the time-increment used.

Even at a POLYDIPROBE concentration as low as 1 μM, a triexponential decay function is needed to simultaneously describe the decay data over the whole emission range. Analyzing at the fluorescence decays at the different wavelengths, however, shows two domains. The emissions at 375 and 395 nm, where only the locally excited states emit, can be fit by a biexponential decay function, while at the two longer wavelengths (480 and 500 nm) it is described by a triexponential decay function, Table 1. The emission at 500 nm solely stems from the excited state pyrene−pyrene interactions.

Compared with the preceding investigations on PROBE[61] and POLYPROBE,[62] one finds an important difference: the sums of the preexponential factors at 480 and 500 nm do not equal zero in the POLYDIPROBE system; see Table 1B. As the sum is not zero, it can be concluded that the excimers are not formed solely via dynamic excited-state processes, and the formation to some extent via direct excitation of ground-state dimers cannot be completely ruled out. This means that no *a priori* information on $\tilde{\mathbf{b}}$ is available.

Table 1. Decay Times of the Charged Fluorescent Probe POLYDIPROBE, Estimated by Global Biexponential Analysis (A) and Global Triexponential Analysis (B, C)[a]

(A)	τ_1 (ns)	τ_2 (ns)	χ_g^2	$Z(\chi_g^2)$
	14.1 ± 0.2	178.1 ± 0.4	1.10	2.1

(B)	τ_1 (ns)	τ_2 (ns)	τ_3 (ns)	χ_g^2	$Z(\chi_g^2)$
	7.3 ± 0.8	50.7 ± 0.5	156.4 ± 0.3	1.02	0.5

λ_{em} (nm)	α_1	α_2	α_3
	time increment = 1.185 ns/channel		
480	−0.022 ± 0.006	−0.407 ± 0.004	0.754 ± 0.002
500	−0.087 ± 0.005	−0.448 ± 0.005	0.713 ± 0.002
	time increment = 408 ps/channel		
480	−0.004 ± 0.002	−0.099 ± 0.001	0.182 ± 0.001
500	−0.013 ± 0.001	−0.106 ± 0.001	0.163 ± 0.001

(C)	τ_1 (ns)	τ_2 (ns)	τ_3 (ns)	χ_g^2	$Z(\chi_g^2)$
	13.5 ± 0.3	51 ± 1	156.2 ± 0.5	1.05	2.0

[a] The biexponential analysis was performed on decay data collected at 375 and 395 nm, where only the two locally excited states emit, while the triexponential analysis was performed on data collected at (B) 480 and 500 nm (decay times and preexponential factors α) or (C) at all four emission wavelengths. The time increments were 408 ps/channel and 1.185 ns/channel.

The fact that biexponential decay traces are observed for the POLYDIPROBE system at emission wavelengths where the locally excited states emit implies that both k_{13} and k_{23} equal zero. The same was found for the PROBE and POLYPROBE studies.[61,62] The photophysical system can thus be described by the model depicted in Scheme 3. Unique values of six rate constants of that scheme have to be determined for the system to be indentifiable. Since there are only two equations available, i.e., eqs 15, only two unknown rate constants can be uniquely determined.

4.3. Scanning the Fluorescence Decay Surface with k_{32} as the Scanned Parameter. Assuming that the deactivation rates determined for PROBE[61] and POLYPROBE[62] can also be used for POLYDIPROBE, provides the values of three rate constants; $k_{01} = 4.38 \times 10^6$ s^{-1}, $k_{02} = 6.66 \times 10^6$ s^{-1}, and $k_{03} = 2 \times 10^7$ s^{-1}. Furthermore, the value of k_{12} as determined for POLYPROBE,[62] i.e., $k_{12} = 1.2 \times 10^8$ s^{-1}, can be used as *a priori* information as well. Still, the value of one rate constant is missing if one wishes to achieve identifiability, and no more *a priori* information is available. By the use of the scanning technique, however, where k_{32} is set at different preset values, the remaining rate constants, i.e., k_{21} and k_{31}, can be determined within certain value boundaries.[47,48,58,62]

To improve the precision of the calculations, data from steady-state emission spectra can be included.[58] It can be concluded that all emission at $\lambda_{em} \geq 500$ nm emanates solely from the excimer state, which means that the emission weight factors for the two other compartments, i.e., $\tilde{c}_1$ and $\tilde{c}_{21}$, can be set equal to zero for $\lambda_{em} \geq 500$ nm.

The scanning analysis of the POLYDIPROBE fluorescence decay data was performed with k_{32} as the scanned parameter. Figure 4 gives the global statistical parameter $Z(\chi^2)$ as a function of k_{32}. Clearly, for 1.6×10^7 s^{-1} < k_{32} < 1.96×10^7 s^{-1}, $Z(\chi^2)$ has acceptable values and the parameter k_{32} has to be confined within these rather narrow limits.

4.4. Limits on the Unknown Rate Constants. There are two different ways to obtain the value boundaries on the two rate constants k_{21} and k_{31}. First,

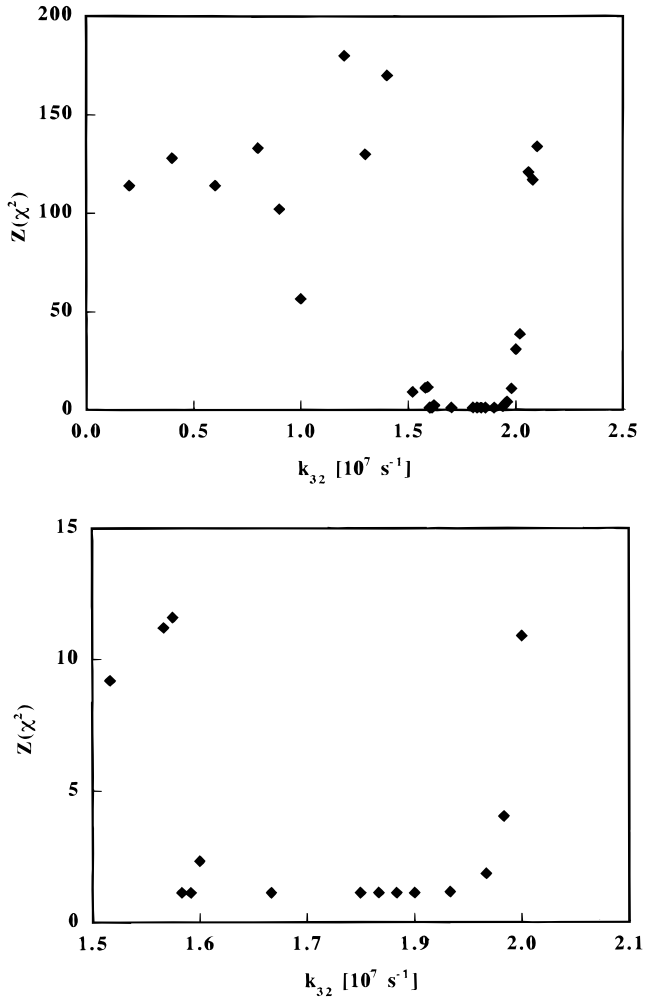

Figure 4. Results of the scanning of the fluorescence decay surface of POLYDIPROBE with k_{32} as the scanned parameter: The *y*-axis gives the statistical parameter $Z(\chi^2)$ as a function of k_{32}.

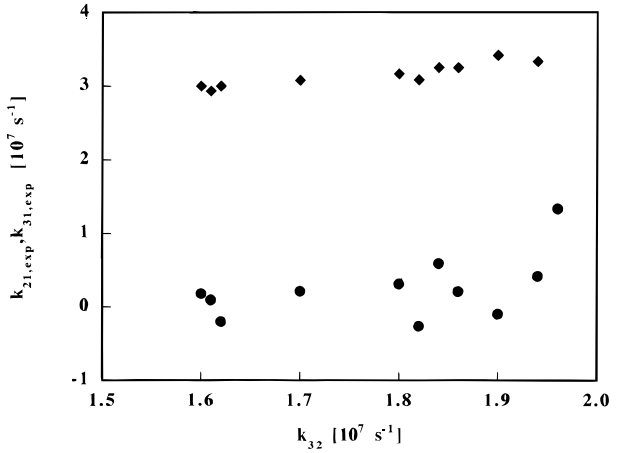

Figure 5. $k_{21,exp}$ (◆) and $k_{31,exp}$ (●) as a function of k_{32}. $k_{21,exp}$ and $k_{31,exp}$ are the values obtained for these parameters in the computer fittings when the scanning of k_{32} is performed. See Table 2 and text for further details.

the obtained values of k_{21} and k_{31} from the fittings, referred to by subscript exp, can be plotted as a function of k_{32}. Such a plot should show within which value boundaries the particular rate constant can vary. These plots, shown in Figure 5, indicate that $k_{21,exp}$ takes almost constant values within the region of interest, while the $k_{31,exp}$ values are very small and vary much

Table 2. Estimated Upper and Lower Limits, Calculated by Two Methods, for the Values of the Rate Constants According to Scheme 3 for POLYDIPROBE in THF[a]

(A) By the Use of Values of $k_{21,exp}$ and $k_{31,exp}$ As Obtained from the Computer Fittings When k_{32} Is Scanned (See Also Text and Figure 5)

$0\ s^{-1} < k_{31,exp} < 6 \times 10^6\ s^{-1}$
$2.9 \times 10^7\ s^{-1} < k_{21,exp} < 3.4 \times 10^7\ s^{-1}$
$1.6 \times 10^7\ s^{-1} < k_{32} < 1.96 \times 10^7\ s^{-1}$

(B) By Calculating the Values of $k_{21,calc}$ and $k_{31,calc}$ from Eqs 15, Using $\overline{S_1 + S_2}$ and $\overline{P - S_1S_2}$ (See Also Text and Figure 6)

$1.32 \times 10^7\ s^{-1} < k_{31,exp} < 1.33 \times 10^7\ s^{-1}$
$1.8 \times 10^7\ s^{-1} < k_{21,exp} < 2.1 \times 10^7\ s^{-1}$
$1.6 \times 10^7\ s^{-1} < k_{32} < 1.96 \times 10^7\ s^{-1}$

[a] The scannings of k_{32} were performed with six known rate constant values ($k_{01} = 4.38 \times 10^6\ s^{-1}$, $k_{02} = 6.66 \times 10^6\ s^{-1}$, $k_{03} = 2 \times 10^7\ s^{-1}$, $k_{12} = 1.2 \times 10^8\ s^{-1}$, $k_{13} = 0\ s^{-1}$, and $k_{23} = 0\ s^{-1}$) and two known emission weight factors.

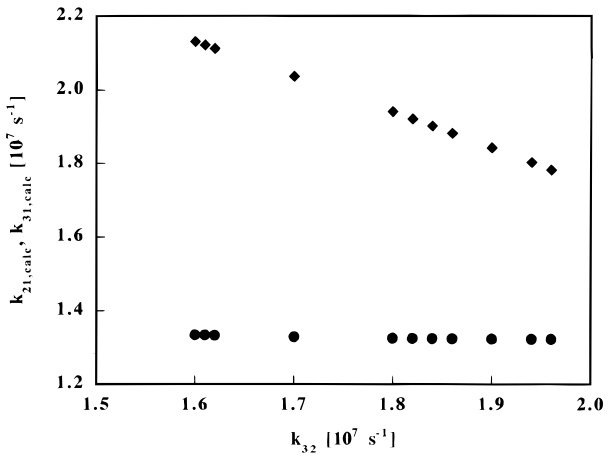

Figure 6. $k_{21,calc}$ (◆) and $k_{31,calc}$ (●) as a function of k_{32}. $k_{21,calc}$ and $k_{31,calc}$ were calculated by the use of $\overline{S_1+S_2}$ and $\overline{P-S_1S_2}$ (eqs 15), respectively. See Table 2 and text for further details.

more. The value boundaries obtained by this method are compiled in Table 2.

Second, the averages $\overline{S_1 + S_2}$ and $\overline{P - S_1S_2}$ can be calculated for k_{32} values within $1.6 \times 10^7\ s^{-1} < k_{32} < 1.96 \times 10^7\ s^{-1}$. The averages obtained are $\overline{S_1 + S_2} = (1.82 \pm 0.04) \times 10^8\ s^{-1}$ and $\overline{P - S_1S_2} = -(1.7 \pm 0.3) \times 10^{15}\ s^{-2}$. Substituting $\overline{S_1 + S_2}$ for $-(\sigma_1 + k_{03})$ and $\overline{P - S_1S_2}$ for σ_3/k_{03} in eqs 15 allows one to calculate k_{21} and k_{31} for each value of the scanned rate constant k_{32}. Plotting these calculated values, referred to by subscript calc, as a function of k_{32} should yield the value boundaries on the rate constants. $k_{21,calc}$ and $k_{31,calc}$ *vs* k_{32} are shown in Figure 6, and the estimated value boundaries are given in Table 2.

It is possible to compare the obtained result on the rate constant of ring-closure with what could be expected for a diffusion-controlled reaction. The magnitude of the second-order rate constant for such a process can be calculated by the Smoluchowski−Stokes−Einstein equation:[73]

$$k_d = \frac{8000RT}{3\eta}\ M^{-1}\ s^{-1} \qquad (18)$$

Although eq 18 is only strictly valid for homogeneous solutions, similar approaches to correlate monomolecular mobility with diffusion-controlled rates have been performed for micellar systems[74−78] as well as for end-to-end motions in polymer systems.[40,42,79,80] Equation 18 allows an estimation of the magnitude of the diffusion-controlled limit of the ring-closure process of POLYDIPROBE.

The viscosity η of THF[81] at 20 °C is 5.5×10^{-4} N s m^{-2}, and the corresponding diffusion-controlled limit will be $k_d = 1.2 \times 10^{10}\ M^{-1}\ s^{-1}$. Setting the radius of gyration of POLYDIPROBE in THF equal to that of poly(ethylene oxide) of the same molecular weight in water, which is an acceptable assumption when comparing poly(alkylene oxides),[82] gives $R_g = 73$ Å.[83] Each POLYDIPROBE has two end groups, yielding the local concentration of ionic end groups to be 2.04 mM, and the first-order limit of the diffusion-controlled ring closure can be calculated to be $2.5 \times 10^7\ s^{-1}$. This value is in very good agreement with the value boundaries on the rate constant k_{21}, Table 2, strongly indicating that the excited-state ring closure indeed is a diffusion-controlled process.

Furthermore, the calculated value of the diffusion-controlled limit and the value of the second-order rate constant k_{21} for POLYPROBE,[62] i.e., $1.3 \times 10^{10}\ M^{-1}\ s^{-1}$, allows the calculation of the POLYDIPROBE concentration at which the intra- and intermolecular aggregations balance. At approximately 1 mM POLYDIPROBE, the probability of intramolecular ring closure and intermolecular aggregation will be equal. The POLYDIPROBE concentration in this study, i.e., 1 μM, is well below this limit, and no intermolecular interactions are observed.

5. Conclusions

By the successive use of data obtained from model compounds, it is possible to unravel even complicated systems undergoing three-state excited-state processes. Following such a strategy, one has to establish the reliability of the obtained model compound results in each subsequent step.

Previously, the photophysics of the charged fluorescent probe PROBE[61] and the monosubstituted poly(tetrahydrofuran) fluorescent probe POLYPROBE[62] was investigated. The decay rate from the unaggregated locally excited state took the same value for POLYPROBE as for PROBE, proving that the presence of the poly(THF) chain does not influence the excited-state photophysics of the chromophore moiety. Furthermore, measurements when a poly(THF) substituted with one quaternary ammonium salt unit was used as added salt gave the deactivation rate of the ion−ion aggregated locally excited state and measurements in function of the POLYPROBE concentration yielded the deactivation rate from the POLYPROBE excimer state. It was observed for PROBE, as well as for POLYPROBE, that the dissociation from the excimer state to the two locally excited states is negligible.

In this study, the results from PROBE[61] and POLYPROBE[62] were used to analyze the fluorescence decay of bis[(*N*,*N*-dimethyl-*N*-[3-(1-pyrenyl)propyl]ammonio)-trifluoromethanesulfonate]-end-capped poly(tetrahydrofuran) (POLYDIPROBE) at low POLYDIPROBE concentration. Stationary emission measurements show that, even at high concentration of added quaternary ammonium salt, there will always be emission detected from the excimer state. This intramolecular excimer formation competes with the ion−ion aggregation. At low POLYDIPROBE concentration, where all reactions can be assumed to be intramolecular, the fluorescence decay is triexponential—thus, the system consists of three different excited states; two locally excited states

of which one is ring-closed ion−ion aggregated and the other open and unaggregated and one excimer state. At those wavelengths where only the locally excited states emit, the emission decays biexponentially, showing that the dissociation of the excimer state to the two locally excited states is negligibly slow. This makes it possible to analyze the fluorescence decay surface according to the scanning technique. The calculations indicate that the ring closure of POLYDIPROBE in THF is close to diffusion-controlled.

Acknowledgment. J.v.S is a postdoctoral fellow at the K. U. Leuven and thanks K. U. Leuven for a postdoctoral grant. N. B. is an *Onderzoeksdirecteur* of the Belgian *Fonds voor Geneeskundig Wetenschappelijk Onderzoek (FGWO).* The continuing support of the Belgian *Fonds voor Kollektief Fundamenteel Onderzoek* and the Ministry of Scientific Programming through IUAP/PAI-IV/11 is gratefully acknowledged. Professor Ph. Teyssié is acknowledged for his continuing interest in this research. Sigrid Depaemelaere and Steven De Backer are thanked for the careful maintenance of the single photon counting systems, and Andrzej Molski is thanked for help with the interpretation of the kinetic data.

References and Notes

(1) MacKnight, W. R.; Earnest, T. *Macromol. Rev.* **1981**, *16*, 41.
(2) Eisenberg, A., Bailey, F. E., Eds. *Coulumbic Interactions in Macromolecular Systems*; ACS Symposium Series 302; American Chemical Society: Waschington, DC, 1986.
(3) Lundberg, R. D. In *Structure and Properties of Ionomers*; Pineri, M., Eisenberg, A., Eds.; NATO ASI Series; D. Reidel: Dordrecht, The Netherlands, 1987; p 387.
(4) Jérôme, R. In *Structure and Properties of Ionomers*; Pineri, M., Eisenberg, A., Eds.; NATO ASI Series; D. Reidel: Dordrecht, 1987; p 399.
(5) Bockris, J.; Reddy, A. *Modern Electrochemistry*; Plenum Press: New York, 1970.
(6) Hara, M.; Lee, A. H.; Wu, J. *J. Polym. Sci., Part B: Polym. Phys.* **1987**, *25*, 1407.
(7) Tanaka, F. *Macromolecules* **1988**, *21*, 2189.
(8) Hara, M.; Wu, J.; Lee, A. *Macromolecules* **1989**, *22*, 754.
(9) Kocak, H. I.; Aras, L. *Polymer* **1990**, *31*, 1328.
(10) Lantman, C. W.; MacKnight, W. J.; Peiffer, D. G.; Sinha, S. K.; Lundberg, R. D. *Macromolecules* **1987**, *20*, 1096.
(11) Hara, M.; Wu, J.; Lee, A. *Macromolecules* **1988**, *21*, 2214.
(12) Pedley, A. M.; Higgins, J. S.; Peiffer, D. G.; Burchard, W. *Macromolecules* **1990**, *23*, 1434.
(13) Lantman, C. W.; MacKnight, W. J.; Peiffer, D. G.; Sinha, S. K.; Lundberg, R. D. *Macromolecules* **1988**, *21*, 1339.
(14) Gabrys, B.; Higgins, J. S.; Lantman, C. W.; MacKnight, W. J.; Pedley, A. M.; Peiffer, D. G.; Rennie, A. R. *Macromolecules* **1989**, *22*, 3746.
(15) Pedley, A. M.; Higgins, J. S.; Peiffer, D. G.; Rennie, A. R. *Macromolecules* **1989**, *22*, 3746.
(16) Register, R. A.; Cooper, S. L.; Thiyagarajan, P.; Chakrapani, S.; Jérôme, R. *Macromolecules* **1990**, *23*, 2978.
(17) Feng, D.; Wilkes, G. L. *Macromolecules* **1991**, *24*, 6788.
(18) Dowling, K. C.; Thomas, J. K. *Macromolecules* **1991**, *24*, 4123.
(19) Otacka, E. P.; Hellman, M. Y.; Blyler, L. L. *J. Appl. Phys.* **1969**, *40*, 4221.
(20) Broze, G.; Jérôme, R.; Teyssié, Ph. *Macromolecules* **1982**, *15*, 920.
(21) Broze, G.; Jérôme, R.; Teyssié, Ph. *Macromolecules* **1982**, *15*, 1300.
(22) Hara, M.; Wu, J. *Macromolecules* **1988**, *21*, 402.
(23) Hara, M.; Wu, J. L.; Jérôme, R.; Granville, M. *Macromolecules* **1988**, *21*, 3331.
(24) Weill, G. *Biophys. Chem.* **1991**, *41*, 1.
(25) Misra, S.; Nguyen-Misra, M.; Mattice, W. L. *Macromolecules* **1994**, *27*, 5037.
(26) Broze, G.; Jérôme, R.; Teyssié, Ph.; Marco, C. *Macromolecules* **1983**, *16*, 996.
(27) Jérôme, R.; Broze, G.; Teyssié, Ph. In *Microdomains in Polymer Solutions*; Dubin, P., Ed.; Plenum Press: New York, 1985; *Polym. Sci. Technol.* **1985**, *30*, 243.
(28) Jérôme, R.; Henrioulle-Granville, M.; Boutevin, B.; Robin, J. J. *Prog. Polym. Sci.* **1991**, *16*, 837.
(29) Granville, M.; Jérôme, R.; Teyssié, Ph.; De Schryver, F. C. *Macromolecules* **1988**, *21*, 2894.
(30) Morawetz, H. *Acc. Chem. Res.* **1994**, *27*, 174.
(31) Goldenberg, M.; Emert, J.; Morawetz, H. *J. Am. Chem. Soc.* **1978**, *100*, 7171.
(32) Zachariasse, K. A.; Duveneck, G.; Busse, R. *J. Am. Chem. Soc.* **1984**, *106*, 1045.
(33) Goedeweeck, R.; De Schryver, F. C. *Photochem. Photobiol.* **1983**, *39*, 515.
(34) Kanaya, T.; Goshiki, K.; Yamamoto, M.; Nishijima, Yö. *J. Am. Chem. Soc.* **1982**, *104*, 3580.
(35) Snare, M. J.; Thistlethwaite, P. J.; Ghiggino, K. P. *J. Am. Chem. Soc.* **1983**, *105*, 3328.
(36) Goedeweeck, R.; Van der Auweraer, M.; De Schryver, F. C. *J. Am. Chem. Soc.* **1985**, *107*, 2334.
(37) Zachariasse, K. A.; Duveneck, G. *J. Am. Chem. Soc.* **1987**, *109*, 3790.
(38) Reynders, P.; Kühnle, W.; Zachariasse, K. A. *J. Am. Chem. Soc.* **1990**, *112*, 3929.
(39) Reynders, P.; Kühnle, W.; Zachariasse, K. A. *J. Phys. Chem.* **1990**, *94*, 4073.
(40) Yekta, A.; Duhamel, J.; Adiwidjaja, H.; Brochard, P.; Winnik, M. A. *Langmuir* **1993**, *9*, 881.
(41) Yekta, A.; Duhamel, J.; Brochard, P.; Adiwidjaja, H.; Winnik, M. A. *Macromolecules* **1993**, *26*, 1829.
(42) Yekta, A.; Xu, B.; Duhamel, J.; Adiwidjaja, H.; Winnik, M. A. *Macromolecules* **1995**, *28*, 956.
(43) Ameloot, M.; Boens, N.; Andriessen, R.; Van den Bergh, V.; De Schryver, F. C. *J. Phys. Chem.* **1991**, *95*, 2041.
(44) Andriessen, R.; Ameloot, M.; Boens, N.; De Schryver, F. C. *J. Phys. Chem.* **1992**, *96*, 314.
(45) Boens, N.; Andriessen, R.; Ameloot, M.; Van Dommelen, L.; De Schryver, F. C. *J. Phys. Chem.* **1992**, *96*, 6331.
(46) Boens, N.; Ameloot, M.; Hermans, B.; De Schryver, F. C.; Andriessen, R. *J. Phys. Chem.* **1993**, *97*, 799.
(47) Boens, N.; Van Dommelen, L.; Ameloot, M. *Biophys. Chem.* **1993**, *48*, 301.
(48) Van Dommelen, L.; Boens, N.; Ameloot, M.; De Schryver, F. C.; Kowalczyk, A. *J. Phys. Chem.* **1993**, *97*, 11738.
(49) Van den Bergh, V.; Kowalczyk, A.; Boens, N.; De Schryver, F. C. *J. Phys. Chem.* **1994**, *98*, 9503.
(50) van Stam, J.; De Feyter, S.; Boens, N.; De Schryver, F. C. *J. Chem. Soc., Chem. Comm.* **1995**, 2433.
(51) Van Dommelen, L.; Boens, N.; Ameloot, M.; De Schryver, F. C. *J. Phys. Chem.* **1995**, *99*, 8959.
(52) Boens, N.; Kowalczyk, A.; Cielen, E. *J. Phys. Chem.*. **1996**, *100*, 4879.
(53) Andriessen, R.; Boens, N.; Ameloot, M.; De Schryver, F. C. *J. Phys. Chem.* **1991**, *95*, 2047.
(54) Khalil, M. M. H.; Boens, N.; De Schryver, F. C. *J. Phys. Chem.* **1993**, *97*, 3111.
(55) Van den Bergh, V.; Boens, N.; De Schryver, F. C.; Ameloot, M.; Steels, P.; Gallay, J.; Vincent, M.; Kowalczyk, A. *Biophys. J.* **1995**, *68*, 1110.
(56) Van den Bergh, V.; Boens, N.; De Schryver, F. C.; Gallay, J.; Vincent, M. *Photochem. Photobiol.* **1995**, *61*, 442.
(57) Meuwis, K.; Boens, N.; De Schryver, F. C.; Gallay, J.; Vincent, M. *Biophys. J.* **1995**, *68*, 2469.
(58) van Stam, J.; Van Dommelen, L.; Boens, N.; Zachariasse, K.; De Schryver, F.C. *J. Phys. Chem.* **1995**, *99*, 9386.
(59) van Stam, J.; De Feyter, S.; De Schryver, F. C.; Evans, C. H. *J. Phys. Chem.* **1996**, *100*, 19959.
(60) Hermans, E.; De Schryver, F. C.; Dutt, G. Bhaskar; van Stam, J.; De Feyter, S.; Boens, N.; Miller, R. D. *New J. Chem.* **1996**, *20*, 829.
(61) Hermans, B.; De Schryver, F. C.; Boens, N.; Ameloot, M.; Jérôme, R.; Teyssié, Ph.; Goethals, E.; Schacht, E. *J. Phys. Chem.* **1994**, *98*, 13583.
(62) Hermans, B.; De Schryver, F. C.; van Stam, J.; Boens, N.; Jérôme, R.; Teyssié, Ph.; Trossaert, G.; Goethals, E.; Schacht, E. *Macromolecules* **1995**, *28*, 3380.
(63) Boens, N.; Janssens, L. D.; De Schryver, F. C. *Biophys. Chem.* **1989**, *33*, 77.
(64) Khalil, M. M. H.; Boens, N.; Van der Auweraer, M.; Ameloot, M.; Andriessen, R.; Hofkens, J.; De Schryver, F. C. *J. Phys. Chem.* **1991**, *95*, 9375.
(65) Boens, N.; Ameloot, M.; Yamazaki, I.; De Schryver, F. C. *Chem. Phys.* **1988**, *121*, 73.
(66) Knutson, J. R.; Beechem, J. M; Brand, L. *Chem. Phys. Lett.* **1983**, *102*, 501.
(67) Löfroth, J.-E. *Anal. Instrum.* **1985**, *14*, 403.
(68) Löfroth, J.-E. *Eur. Biophys. J.* **1985**, *13*, 45.

(69) Reekmans, S.; Boens, N.; Van der Auweraer, M.; Luo, H.; De Schryver, FC. *Langmuir* **1989**, *5*, 948.
(70) Janssens, L. D.; Boens, N.; Ameloot, M.; De Schryver, F. C. *J. Phys. Chem.* **1990**, *94*, 3564.
(71) Marquardt, D. W. *J. Soc. Ind. Appl. Math.* **1963**, *11*, 431.
(72) Boens, N. In *Luminescence Techniques in Chemical and Biochemical Analysis*; Baeyens, W. R. G.; De Keukeleire, D., Korkidis, K., Eds.; Marcel Dekker: New York, 1991; p 21.
(73) Rice, S. In *Comprehensive Chemical Kinetics*; Bamford, C. H., Tipper, C. F. H., Compton, R. G., Eds.; Elsevier: Amsterdam, 1985; p 3.
(74) Van der Auweraer, M.; Dederen, C.; Palmans-Windels, C.; De Schryver, F. C. *J. Am. Chem. Soc.* **1982**, *104*, 1800.
(75) Van der Auweraer, M.; De Schryver, F. C. *Chem. Phys.* **1987**, *111*, 105.
(76) Van der Auweraer, M., Roelants, E., Verbeeck, A., De Schryver, F. C., Eds. *Surfactants in Solution 7*; Plenum: New York, 1989; pp 141−157.
(77) Almgren, M.; Alsins, J. *Isr. J. Chem.* **1991**, *31*, 159.
(78) Almgren, M.; Alsins, J.; Jóhannsson, R.; Mukhtar, E. *Proc. Indian Acad. Sci.* **1992**, *104*, 275.
(79) Yekta, A.; Duhamel, J.; Winnik, M. A. *J. Chem. Phys.* **1992**, *97*, 1554.
(80) Martinho, J. M. G.; Castanheira, E. M. S.; Reis e Sousa, A. T.; Saghbini, S.; André, J. C.; Winnik, M. A. *Macromolecules* **1995**, *28*, 1167.
(81) *Handbook of Chemistry and Physics*, 73rd ed.; Chemical Rubber Co.: Boca Raton, FL, 1992.
(82) Brandrup, J., Immergut, E. H., Eds. *Polymer Handbook*; John Wiley: New York, 1989.
(83) Abrahmsén-Alami, S.; Stilbs, P. *J. Phys. Chem.* **1994**, *98*, 6359.

MA961271Q